Reexamination of the decoherence of spin registers

Jan Tuziemski,[1,2,3,*] Aniello Lampo,[4] Maciej Lewenstein,[4,5] and Jarosław K. Korbicz[6]

[1]*Faculty of Applied Physics and Mathematics, Technical University of Gdańsk, 80-233 Gdańsk, Poland*
[2]*National Quantum Information Center of Gdańsk, 81-824 Sopot, Poland*
[3]*Department of Physics, Stockholm University, Stockholm SE-106 91, Sweden*
[4]*ICFO – Institut de Ciències Fotòniques, The Barcelona Institute of Science and Technology, 08860 Castelldefels (Barcelona), Spain*
[5]*ICREA, Psg. Lluis Companys 23, E-08010 Barcelona, Spain*
[6]*Center for Theoretical Physics, Polish Academy of Sciences, Aleja Lotników 32/46, 02-668 Warsaw, Poland*

We revisit the decoherence process of a multiqubit register interacting with a thermal bosonic bath. We generalize the previous studies by considering not only the register's behavior but also a part of its environment. In particular, we are interested in information flow from the register to the environment, which we describe using recently introduced multipartite quantum state structures called spectrum broadcast structures. Working in two specific cases of (i) two-qubit register and (ii) collective decoherence, we identify the regimes where the environment acquires almost complete information about the register state. We also study in more detail the interesting causal aspects related to the finite propagation time of the field disturbances between the qubits. Finally, we describe quantum state structures which appear due to the presence of protected spaces.

I. INTRODUCTION

Decoherence of qubit registers due to an interaction with a thermal bath is a seemingly well-studied process [1,2] with all the relevant timescales and protected spaces identified. The importance of such studies lies in quantum technological applications and in the general understanding of the foundations of quantum physics. However, only the register's dynamics was studied, with the environment treated merely as the source of noise. On the other hand, it emerges from a recent studies under the names of quantum Darwinism [3] and spectrum broadcast structures (SBS) [4,5] that, during the decoherence, the environment can gain valuable information about the system and play the role of a communication channel. This role is of a great importance for the understanding of the quantum-to-classical transition, touching such deep questions as that of objectivity (see, e.g., [3,5]). Recently, the environment as a communication channel has been studied for a single qubit interacting with a thermal bath (the spin-boson model) [6]. In particular, the regimes of SBS formation were identified and the relation to non-Markovianity analyzed. In this work, we complement those studies with a similar analysis of a spin register in a thermal bosonic bath (see [7] for the studies of a spin environment). It can also be regarded as a generalization of the previous works [1,2] to include (a part of) the environment.

Generalization from a single qubit to a multiqubit register, in which the register qubits do not directly interact with each other, brings some remarkable qualitative changes. First of all, as it is well known there appear so-called decoherence-free subspaces (DFS), which are protected subspaces of the register, immune to decoherence. When the environment is included, there appears a complementary notion of so-called orthogonalization-free subspaces (OFS), for which the environment information gain is zero [7]. We show here an example of a simultaneous DFS and OFS, which has some nontrivial consequences for the joint system-environment state. Second, the spacial separation of qubits introduces new, with respect to the single qubit case, effects corresponding to a nonzero time-of-flight of the bosonic field disturbances between the physical locations of qubits. Known for a long time for the register qubits [2,8,9], here they are studied for the environment and from the quantum information perspective. In particular, studying a two-qubit register we show that a decohering-recohering impulse felt by the register is accompanied by a similar information gain or loss impulse in fragments of the environment.

The physics discussed in this paper is very much related to the physics of Dicke's superradiance [10]. In particular, collective effects occurring in multiqubit registers correspond directly to superradiant effects and radiation trapping effects. More concretely, when two emitters are close one to another and their dipoles oscillate in phase, the constructive interference leads to superradiance, i.e., the effect that the radiation rate is twice as big as the rate for a single emitter. Conversely, if the dipoles oscillate in antiphase, the destructive interference takes place, the radiation rate goes to zero, and the radiation is trapped. In the decoherence language, this corresponds to a formation of a decoherence-free subspace. The effects of constructive and destructive interference are still present when the emitters are separated. The photon emitted by one emitter affects the second one in an constructive or destructive manner, depending on whether their dipole moments are in phase or out of phase, respectively.

The main tool used here to study information flow is the so-called spectrum broadcast structures, introduced in [4,5].

*jan.tuziemski@pg.edu.pl

Assuming that some fraction of the environment, called fE, is left for observation, SBS are the following multipartite quantum state structures between the central system S and fE:

$$\rho_{S:fE} = \sum_i p_i |x_i\rangle\langle x_i| \otimes \rho_i^{E_1} \cdots \otimes \rho_i^{E_{fN}}, \qquad (1)$$

$$\rho_i^{E_k} \perp \rho_{i'}^{E_k} \text{ for every } i' \neq i \text{ and } k = 1, \ldots, fN. \qquad (2)$$

Here $\{|x_i\rangle\}$ is the so-called pointer basis of the register to which it decoheres, p_i are initial pointer probabilities, and $\rho_i^{E_k}$ are some states of the observed parts of the environment with mutually orthogonal supports for different pointer indexes i. The state (1) describes redundantly stored information about the system, the index i, in the environment. Because of that, it corresponds to a certain operational form of objectivity of the central system's state [5]. It has been shown to appear in a variety of models, such as the illuminated sphere model [4], the spin-boson model [6], the quantum Brownian motion model [11–13], a simplified quantum electrodynamics model [14], in a recently proposed mechanism of gravitational decoherence [15], as well as in generic von Neumann measurements [16]. The structure (1) is an idealized structure, and in realistic situations one can expect only some form of an approach to it. This approach has been characterized mathematically in [17] (see also [4]) in terms of two quantities: the usual decoherence factors and state fidelities [18] between the environmental states $\rho_i^{E_k}$. These are the central quantities of our analysis.

The work is organized as follows. In Sec. II we recall the register model and its dynamics. In Sec. III we analyze the structure of the partially reduced state $\rho_{S:fE}$ in the model and derive general expressions for the decoherence and fidelity factors, including full analytical solutions for both, assuming the whole frequency spectrum of the environment is taken into the account. Section IV is dedicated to the simplest, nontrivial case—a two-qubit register. In Sec. V we consider another simplified situation—so-called collective decoherence, corresponding to very short transit times of the bosonic field perturbation compared to the other timescales of the model. The conditions for protected subspaces are derived and the consequences for the form of the partially traced state analyzed. Concluding remarks are presented in Sec. VI. In Appendix A we present an analytical derivation of the decoherence factor and state fidelities for uncut environments. We discuss the relation to the Dicke model and the related papers on superradiance and radiation trapping in the Appendix B.

II. THE MODEL AND ITS DYNAMICS

We study the model of an L-qubit register interacting with a bosonic environment. The system is described by the following Hamiltonian [1,2]:

$$H = H_S + H_E + H_{\text{int}}, \qquad (3)$$

where the free dynamics of the register and the environment is given by

$$H_S = \sum_{n=1}^{L} J_z^{(n)}, \quad H_E = \sum_k \omega_k a_k^\dagger a, \qquad (4)$$

with $J_z^{(n)} = \frac{1}{2}\sigma_z$ being the Pauli σ_z operator acting on the nth register qubit. The interaction between the qubits and the environment modes is of a form

$$H_{\text{int}} = \sum_{n=1}^{L} J_z^{(n)} \otimes \sum_k \left(g_k^n a_k^\dagger + g_k^{n*} a_k \right). \qquad (5)$$

This kind of interaction appears naturally when one considers an ensemble of two-level atoms coupled to the electromagnetic (EM) field. Usually in such systems, the free Hamiltonian of atoms is described by the sum of the σ_z matrices, describing projections on the ground and excited states, multiplied by the corresponding energies. The dipolar coupling with the EM field is then described by σ_x or σ_y matrices. In the special situations when the ground and excited states are degenerated, the free Hamiltonian vanishes and we have to "rotate" the interaction term so that it contains the diagonal σ_z matrices.

Since $[J_z^{(n)}, H] = 0$, there is no energy transfer between the register and the environment, and thus dissipation is not taken into account. This means that our approach is valid as long as the dissipation timescale is much larger than timescales of processes that we are interested in, what is usually the case. To derive the evolution operator it is convenient to work in the interaction picture, with the interaction Hamiltonian given by

$$H_{\text{int}}^I(t) = \sum_n J_z^{(n)} \otimes \sum_k \left(g_k^n a_k^\dagger e^{i\omega_k t} + g_k^{n*} a_k e^{-i\omega_k t} \right). \qquad (6)$$

From the above expression we can easily derive the unitary evolution of the whole system $\hat{U}_{S:E}^I(t)$, using, e.g., the Magnus expansion. To present the results we introduce the following notation (cf. [6]): (i) the register state is determined by a bit string vector $\boldsymbol{\epsilon} \equiv (\epsilon_1, \ldots, \epsilon_L)$, where $\epsilon_n \equiv \pm\frac{1}{2}$; (ii) for the kth field mode the coupling constants are also arranged into a vector $\boldsymbol{g_k} \equiv (g_k^1, \ldots, g_k^L)$. We then arrive at

$$\hat{U}_{S:E}^I(t) = \sum_{\boldsymbol{\epsilon}} |\boldsymbol{\epsilon}\rangle\langle\boldsymbol{\epsilon}| \otimes \bigotimes_k \hat{U}_k^I(t; \boldsymbol{\epsilon}), \qquad (7)$$

$$\hat{U}_k^I(t; \boldsymbol{\epsilon}) \equiv \hat{D}(\alpha_k(t)\boldsymbol{\epsilon} \cdot \boldsymbol{g_k}) e^{i|\boldsymbol{\epsilon} \cdot \boldsymbol{g_k}|^2 \xi_k(t)}, \qquad (8)$$

$$\alpha_k(t) \equiv \frac{1 - e^{i\omega_k t}}{\omega_k}, \qquad (9)$$

$$\xi_k(t) \equiv \frac{\omega_k t - \sin(\omega_k t)}{\omega_k^2}. \qquad (10)$$

Above, $\hat{D}(\beta_k) \equiv e^{\beta_k a_k^\dagger - \beta_k^* a_k}$ is the multimode displacement operator. In accord with the quantum Darwinism – spectrum broadcasting scenario, we are interested in a situation where some of environmental degrees of freedom are left for observation while other pass unobserved and hence can be traced out.

III. THE STRUCTURE OF THE PARTIALLY REDUCED STATE – GENERAL CONSIDERATIONS

Our main object of study is thus what we call a partially reduced state,

$$\rho_{S:fE}(t) = \text{tr}_{(1-f)E} \rho_{S:E}(t), \qquad (11)$$

where we denote symbolically by fE the observed fraction of the environment, consisting of fN modes, $0 < f < 1$, $(1 - f)E$ represents the unobserved fraction of $(1 - f)N$ modes, and $\rho_{S:E}(t) = \hat{U}_{S:E}(t)\rho_{S:E}(0)\hat{U}_{S:E}(t)$ is the evolved state of the full $S : E$ system. At this moment we leave the fractions fE and $(1 - f)E$ unspecified and will study how the partially traced state depends on them in what follows.

Assuming the usual full product initial state $\rho_{S:E}(0) = \rho_{0S} \otimes \bigotimes_k \rho_{0k}$, a quick calculation gives

$$\rho^I_{S:fE}(t) = \sum_{\epsilon} c_{\epsilon\epsilon}|\epsilon\rangle\langle\epsilon| \otimes \bigotimes_k^{fN} \rho^I_k(t;\epsilon)$$
$$+ \sum_{\epsilon}\sum_{\epsilon'\neq\epsilon} \gamma_{\epsilon\epsilon'}(t)c_{\epsilon\epsilon'}|\epsilon\rangle\langle\epsilon'|$$
$$\otimes \bigotimes_k^{fN} U^I_f(t;\epsilon)\rho_{0k}\hat{U}^I_f(t;\epsilon')^{\dagger}, \quad (12)$$

where $c_{\epsilon\epsilon'} \equiv \langle\epsilon|\rho_{0S}|\epsilon'\rangle$,

$$\rho^I_k(t;\epsilon) \equiv \hat{U}^I_k(t;\epsilon)\rho_{0k}\hat{U}^I_k(t;\epsilon)^{\dagger}, \quad (13)$$

$$\gamma_{\epsilon\epsilon'}(t) \equiv \prod_{k\in(1-f)E} tr\big[\hat{U}^I_k(t;\epsilon)\rho_{0k}\hat{U}^I_k(t;\epsilon')\big], \quad (14)$$

the last being the decoherence factor responsible for suppression of the register's off-diagonal terms in the $|0,1\rangle^{\otimes L}$ basis, serving here as the register's pointer basis. Assuming that the environment is initially in a thermal state, the decoherence factor can be compactly written in a matrix form as

$$-\ln\gamma_{\epsilon\epsilon'}(t) = \Delta\epsilon^T\mathbf{\Gamma}(t)\Delta\epsilon + i[\epsilon^T\mathbf{\Gamma}^+(t)\epsilon$$
$$- \epsilon'^T\mathbf{\Gamma}^+(t)\epsilon' - 2\epsilon^T\mathbf{\Gamma}^-(t)\epsilon'], \quad (15)$$

where $\Delta\epsilon \equiv \epsilon - \epsilon' = (\epsilon_1 - \epsilon'_1, \ldots, \epsilon_L - \epsilon'_L)$ is vector of the differences. We note that unlike in the single-qubit case [19,20], here the decoherence factor has both real and imaginary parts [1,2]. Clearly, the vanishing of the real-phase part,

$$-\ln\Gamma_{\epsilon\epsilon'}(t) \equiv \Delta\epsilon^T\mathbf{\Gamma}(t)\Delta\epsilon, \quad (16)$$

implies a decay of the off-diagonal elements and in what follows we will study this part. To further specify the above matrices, we assume a wavelike position-dependent form of the coupling, reflecting the wavelike character of the bosonic modes. This can be thought as, e.g., assuming that the interactions of the register with the EM field can be well described using the dipole approximation, where the coupling depends only on the positions of the register qubits but not on their internal electronic degrees of freedom:

$$\mathbf{g}_k = g_k(e^{-i\mathbf{k}\mathbf{r}_1}, \ldots, e^{-i\mathbf{k}\mathbf{r}_L}). \quad (17)$$

Then the elements of matrices entering Eq. (15) are given by [1,2]

$$\mathbf{\Gamma}_{nm}(t) \equiv \frac{1}{2}\sum_{k\in(1-f)E}|g_k\alpha_k(t)|^2\coth\left(\frac{\omega_k}{2k_BT}\right)\cos(\mathbf{k}\Delta\mathbf{r}_{nm}),$$
$$(18)$$

$$\mathbf{\Gamma}^+_{nm}(t) \equiv \sum_{k\in(1-f)E}|g_k|^2\xi_k(t)\cos(\mathbf{k}\Delta\mathbf{r}_{nm}), \quad (19)$$

$$\mathbf{\Gamma}^-_{nm}(t) \equiv \frac{1}{2}\sum_{k\in(1-f)E}|g_k\alpha_k(t)|^2\sin(\mathbf{k}\Delta\mathbf{r}_{nm}), \quad (20)$$

with $\Delta\mathbf{r}_{nm} = \mathbf{r}_n - \mathbf{r}_m$ being the physical distance between the register qubits.

The novelty of our approach compared to standard treatments [1,2] is that we are interested not only in the state of the register, but also in the part of its environment. Especially we will be interested in what, if any, system-related information those observed parts of the environment obtain during the evolution. As a measure of the information content we will choose the state fidelity of the states (13) for different ϵ, ϵ' [4,6]:

$$B^{(k)}_{\epsilon\epsilon'}(t) \equiv tr\sqrt{\sqrt{\rho_k(t;\epsilon)}\rho_k(t;\epsilon')\sqrt{\rho_k(t;\epsilon)}}. \quad (21)$$

Just like in the previous studies [4,6], we will be interested in some sort of a thermodynamic limit with large N and the information content of macroscopic groups of modes rather than of single modes which may contain vanishingly small information about the register [4]. We will thus divide the observed modes into bigger groups called macrofractions $\mathcal{M}$ [4]. We define the observed fraction of the environment to be $fE \equiv \cup^{fM}_{\mathcal{M}=1}mac_{\mathcal{M}}$, with a state of a macrofraction simply defined as

$$\rho_{\mathcal{M}}(t;\epsilon) = \bigotimes_{k\in\mathcal{M}}\rho_k(t,\epsilon). \quad (22)$$

The quantity we will be interested in is thus a macrofraction overlap rather than the microscopic one (21):

$$B^{\mathcal{M}}_{\epsilon\epsilon'}(t) \equiv tr\sqrt{\sqrt{\rho_{\mathcal{M}}(t;\epsilon)}\rho_{\mathcal{M}}(t;\epsilon')\sqrt{\rho_{\mathcal{M}}(t;\epsilon)}}$$
$$= \prod_{k\in\mathcal{M}}tr\sqrt{\sqrt{\rho_k(t;\epsilon)}\rho_k(t;\epsilon')\sqrt{\rho_k(t;\epsilon)}} = \prod_{k\in\mathcal{M}}B^{(k)}_{\epsilon\epsilon'}(t).$$
$$(23)$$

In the considered model the above overlap can be calculated and reads

$$-\ln B^{\mathcal{M}}_{\epsilon\epsilon'}(t) = \Delta\epsilon^T\mathbf{B}^{\mathcal{M}}(t)\Delta\epsilon, \quad (24)$$

where we define a $L \times L$ matrix

$$\mathbf{B}^{\mathcal{M}}_{nm}(t) \equiv \frac{1}{2}\sum_{k\in\mathcal{M}}|g_k\alpha_k(t)|^2\tanh\left(\frac{\omega_k}{2k_BT}\right)\cos(\mathbf{k}\Delta\mathbf{r}_{nm}). \quad (25)$$

Functions $\Gamma_{\epsilon\epsilon'}$, $B^{\mathcal{M}}_{\epsilon\epsilon'}(t)$ are the basic objects of our study. If they simultaneously vanish, the partially traced state approaches the SBS form [17]. We stress that unlike in the case of a single qubit [6], now they are given by matrix expressions, which as we will see will lead to qualitatively different behavior. Instead of working with relative distances and wave vectors, let us introduce transit times τ_{nm}, defined as the times that a signal needs to travel between the nth and mth qubits [2]:

$$\mathbf{k}\Delta\mathbf{r}_{nm} \equiv \omega\tau_{nm}. \quad (26)$$

For example, in the case of a solid-state implementation of the register, the bosonic bath can be usually associated with the

TABLE I. Pairs of states $(|\boldsymbol{\epsilon}\rangle, |\boldsymbol{\epsilon}'\rangle)$ accordingly to their $\Delta\epsilon_1\Delta\epsilon_2$ value. Diagonal elements $(|\boldsymbol{\epsilon}\rangle, |\boldsymbol{\epsilon}\rangle)$ are not taken into account.

$\Delta\epsilon_1\Delta\epsilon_2 = 0$ Single qubit	$\Delta\epsilon_1\Delta\epsilon_2 = -1$ Singlet	$\Delta\epsilon_1\Delta\epsilon_2 = +1$ GHZ-type
$(\lvert\frac{1}{2},\frac{1}{2}\rangle,\lvert\frac{1}{2},-\frac{1}{2}\rangle)$, $(\lvert\frac{1}{2},\frac{1}{2}\rangle,\lvert-\frac{1}{2},\frac{1}{2}\rangle)$, $(\lvert\frac{1}{2},-\frac{1}{2}\rangle,\lvert-\frac{1}{2},-\frac{1}{2}\rangle)$, $(\lvert-\frac{1}{2},\frac{1}{2}\rangle,\lvert-\frac{1}{2},-\frac{1}{2}\rangle)$	$(\lvert\frac{1}{2},-\frac{1}{2}\rangle,\lvert-\frac{1}{2},\frac{1}{2}\rangle)$	$(\lvert\frac{1}{2},\frac{1}{2}\rangle,\lvert-\frac{1}{2},-\frac{1}{2}\rangle)$

phonon field, so the transit time will determine speed of information propagation via phonons [2]. Then, assuming that the fractions of the environment we are working with are large, we pass to the usual continuum limit and introduce spectral density $J(\omega)$. In these terms the elements of decoherence and fidelity matrices take the form

$$\boldsymbol{\Gamma}_{nm}(t) = \int_{(1-f)E} d\omega J(\omega)\frac{1-\cos(\omega t)}{\omega^2}\coth$$
$$\times\left(\frac{\omega}{2k_B T}\right)\cos(\omega\tau_{nm}), \quad (27)$$

$$\boldsymbol{\Gamma}_{nm}^+(t) = \int_{(1-f)E} d\omega J(\omega)\frac{\omega t-\sin(\omega t)}{\omega^2}\cos(\omega\tau_{nm}), \quad (28)$$

$$\boldsymbol{\Gamma}_{nm}^-(t) = \frac{1}{2}\int_{(1-f)E} d\omega J(\omega)\frac{1-\cos(\omega t)}{\omega^2}\sin(\omega\tau_{nm}), \quad (29)$$

$$\boldsymbol{B}_{nm}^{\mathcal{M}}(t) = \int_{\mathcal{M}} d\omega J(\omega)\frac{1-\cos(\omega t)}{\omega^2}\tanh\left(\frac{\omega}{2k_B T}\right)\cos(\omega\tau_{nm}). \quad (30)$$

In the above expressions $(1-f)E$ and $\mathcal{M}$ denote symbolically the sets of unobserved and observed frequencies, respectively. We note that in each of the above matrices all the diagonal entries are equal as the transit times τ_{mn} drop out of the expressions. Moreover, the matrices $\boldsymbol{\Gamma}(t)$, $\boldsymbol{\Gamma}^+(t)$, and $\boldsymbol{B}^{\mathcal{M}}(t)$ are real symmetric, while $\boldsymbol{\Gamma}^-(t)$ is real skew-symmetric. As the spectral density we adopt the usual for the spin-boson model expression:

$$J(\omega) = \frac{\omega^s}{\Lambda^{s-1}}\exp\left[-\omega/\Lambda\right], \quad (31)$$

where Λ is the cut-off frequency and s the Ohmicity parameter.

There are several ways to divide environmental degrees of freedom into observed and unobserved parts [6]. First, one can assume that, due to their large size, both unobserved and observed parts of the environment are described by the full spectral density. We will refer to this case as *uncut* spectral density. In this case the above integrals are solvable analytically. Due to their length, the formulas are presented in Appendix A. Here we will study them numerically in further parts of the manuscript for a two-qubit register.

The second possibility is that the observed and unobserved parts of environment are formed by given parts of the spectrum. This situation can be pictured as an observation of the environment via a narrow band detector (rather than a wide band, as above). We will assume the observed frequencies are formed by a spectral interval $[\alpha, \beta]$ and study the dependence of the decoherence and the state fidelity on the position of the interval. This case will be referred to as *cut* spectral density. Based on the studies from [6], one

can assume a sharp spectral cut, as there is no qualitative difference between the sharp and soft cuts.

Decoherence- and orthogonalization-free subspaces

Depending on the values of the decoherence factor Eq. (15) and state fidelity Eq. (24), the structure of the partially reduced state Eq. (12) may be a good approximation of a SBS. However, it is also possible that, for some states of the register, one of the discussed processes will not take place. In such a case, as in [7], we will say that a subspace $S \subseteq \{\pm\frac{1}{2}\}^L$ exhibits a strong decoherence-free subspace (DFS) property if

$$\forall_{t\in\mathbb{R}_+}\forall_{\boldsymbol{\epsilon},\boldsymbol{\epsilon}'\in S}\gamma_{\boldsymbol{\epsilon}\boldsymbol{\epsilon}'}(t) = 1 \quad (32)$$

and a weak DFS if

$$\forall_{t\in\mathbb{R}_+}\forall_{\boldsymbol{\epsilon},\boldsymbol{\epsilon}'\in S}|\gamma_{\boldsymbol{\epsilon}\boldsymbol{\epsilon}'}(t)| = 1. \quad (33)$$

Similarly, we define an orthogonalization-free subspace to occur when

$$\forall_{t\in\mathbb{R}_+}\forall_{\boldsymbol{\epsilon},\boldsymbol{\epsilon}'\in S}\forall_{\mathcal{M}}B_{\boldsymbol{\epsilon}\boldsymbol{\epsilon}'}^{\mathcal{M}}(t) = 1. \quad (34)$$

In general, due to the fact that expressions for decoherence factor and state fidelity are quite involved, it is not possible to analytically determine which states form DSF or OSF. However, when a register's qubits interact collectively with the environment one may introduce conditions for DSF and OSF. This case is discussed in detail in Sec. V.

IV. TWO-QUBIT REGISTER

A general study of the L-qubit register is quite complicated due to the matrix character of both decoherence factor and state fidelity. Here we study the first nontrivial register, consisting of two qubits, extending the original analysis of [2] from decoherence to SBS. For this case there is only one transit time τ and the real decoherence factor between the register states $|\boldsymbol{\epsilon}\rangle$ and $|\boldsymbol{\epsilon}'\rangle$ reads [cf. (16)]

$$-\ln\Gamma_{\boldsymbol{\epsilon}\boldsymbol{\epsilon}'}(t) = \|\Delta\boldsymbol{\epsilon}\|^2\boldsymbol{\Gamma}_{11}(t) + 2\Delta\epsilon_1\Delta\epsilon_2\boldsymbol{\Gamma}_{12}(t), \quad (35)$$

where $\|\Delta\boldsymbol{\epsilon}\|^2 = (\Delta\epsilon_1)^2 + (\Delta\epsilon_2)^2$. We are interested here only in the real part of (15), as it is sufficient for showing damping of the off-diagonal elements. Similarly, one finds that

$$-\ln B_{\boldsymbol{\epsilon}\boldsymbol{\epsilon}'}^{\mathcal{M}}(t) = \|\Delta\boldsymbol{\epsilon}\|^2\boldsymbol{B}_{11}^{\mathcal{M}}(t) + 2\Delta\epsilon_1\Delta\epsilon_2\boldsymbol{B}_{12}^{\mathcal{M}}(t). \quad (36)$$

As a result, for a two-qubit register, there are three groups of nondiagonal density matrix elements, presented in Table I, responsible for different types of coherence and decohering in a different manner according to the value of $\Delta\epsilon_1\Delta\epsilon_2$. Similarly, the distinguishability of the environmental states depends on $\Delta\epsilon_1\Delta\epsilon_2$ too. We can distinguish the following nontrivial cases:

A. Effectively single-qubit case

This is the case when vectors $\boldsymbol{\epsilon}, \boldsymbol{\epsilon}'$ differ at most at one position, e.g., $\epsilon_1 = \epsilon_1'$, $\epsilon_2 \neq \epsilon_2'$, or equivalently, $\Delta\epsilon_1 \Delta\epsilon_2 = 0$. This subspace is spanned by four states as shown in Table I. One obtains

$$-\ln\Gamma_{\boldsymbol{\epsilon}\boldsymbol{\epsilon}'}(t) = \boldsymbol{\Gamma}_{11}(t) \qquad (37)$$

and

$$-\ln B_{\boldsymbol{\epsilon}\boldsymbol{\epsilon}'}^{\mathcal{M}}(t) = \boldsymbol{B}_{11}^{\mathcal{M}}(t). \qquad (38)$$

In this case, apart from the phase, the register behaves effectively as a single spin interacting with a bosonic bath. Therefore we will refer to it as a "single-qubit" case. This conclusion is not restricted just to a two-qubit register. To see this, consider two states of an L-qubit register that differs at the nth position; then it follows from Eq. (15) that $\ln\Gamma_{\boldsymbol{\epsilon}\boldsymbol{\epsilon}'}(t) = -\boldsymbol{\Gamma}_{nn}(t) = -\boldsymbol{\Gamma}_{11}(t)$, as all the diagonal elements are equal, and a similar result holds for fidelity. A detailed investigation of the SBS formation for a single central spin has been performed in [6] and we refer the reader to that work. Here, we will use this case only as a reference to highlight novel features of the register model. For a fair comparison, we note that the Hamiltonian of the spin-boson model is usually defined using σ_z, and here we used $\frac{1}{2}\sigma_z$, following the common quantum register convention. Consequently, the comparison of the result presented here with those of [6] should take into account that in the spin-boson model Eqs. (37) and (38) read $\ln\Gamma_{\boldsymbol{\epsilon}\boldsymbol{\epsilon}'}(t) = -4\boldsymbol{\Gamma}_{11}(t)$ and $\ln B_{\boldsymbol{\epsilon}\boldsymbol{\epsilon}'}^{\mathcal{M}}(t) = -4\boldsymbol{B}_{11}^{\mathcal{M}}(t)$, respectively.

B. True two-qubit case

The remaining nontrivial case is when the vectors $\boldsymbol{\epsilon}, \boldsymbol{\epsilon}'$ differ at all positions, i.e., $\epsilon_1 \neq \epsilon_1'$, $\epsilon_2 \neq \epsilon_2'$. This situation is described by pairs of states such that $\Delta\epsilon_1 \Delta\epsilon_2 = \pm 1$, see Table I. Then the corresponding expressions take a form

$$-\ln\Gamma_{\boldsymbol{\epsilon}\boldsymbol{\epsilon}'}(t) = 2[\boldsymbol{\Gamma}_{11}(t) + \Delta\epsilon_1\Delta\epsilon_2\boldsymbol{\Gamma}_{12}(t)] \qquad (39)$$

and

$$-\ln B_{\boldsymbol{\epsilon}\boldsymbol{\epsilon}'}^{\mathcal{M}}(t) = 2[\boldsymbol{B}_{11}^{\mathcal{M}}(t) + \Delta\epsilon_1\Delta\epsilon_2\boldsymbol{B}_{12}^{\mathcal{M}}(t)]. \qquad (40)$$

Note that in the Dicke superradiant limit, when $k\Delta r_{nm} = \omega\tau_{nm} \rightarrow 0$, the right-hand side of (39) tends to $4\boldsymbol{\Gamma}_{11}(t)$ or zero, indicating, as expected, superradiance or radiation trapping, respectively. In the latter case there will be a strong DFS [cf. Eq. (32)]. Similarly, $\boldsymbol{B}_{11}^{\mathcal{M}}(t) = \boldsymbol{B}_{12}^{\mathcal{M}}(t)$ and $\Delta\epsilon_1\Delta\epsilon_2 = -1$ leads to an OFS [cf. Eq. (34)]. We will study such cases in more detail in Sec. V, dedicated to collective decoherence.

We perform further studies of Eqs. (39) and (40) numerically. Although for the uncut case we have the analytical formulas in Appendix A, it is more convenient to plot them. In Fig. 1 we present results for the uncut spectral density—the decoherence factor and the fidelity for different values of the transit time τ, rescaled to the cutoff Λ and assuming a moderate temperature $0 \ll T \ll s\Lambda$. In each plot there are two curves corresponding to different values of $\Delta\epsilon_1\Delta\epsilon_2$ and the "single-qubit" case [cf. (37, 38)] for a comparison. One immediately sees that both decoherence and the information gain by the environment are more efficient for a register than
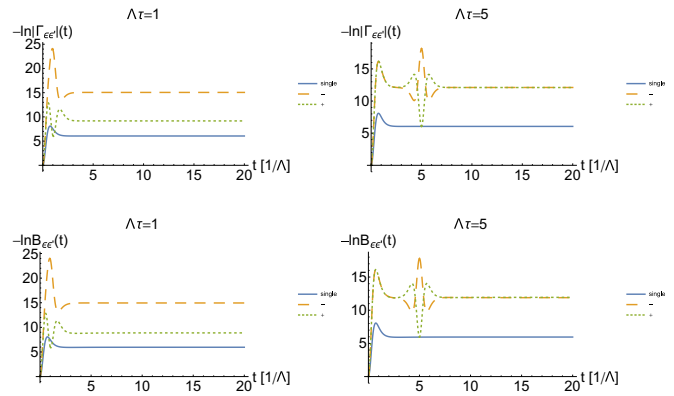

FIG. 1. Uncut spectral density case, different transit times. Logarithm of decoherence factor [Eq. (39)] – upper trace, and fidelity [Eq. (40)] – lower trace for different values of transit time τ [Eq. (26)]: $\Lambda\tau = 1$ - upper left and lower left, $\Lambda\tau = 5$ - upper right and lower right. In each plot there are three curves corresponding to states with different values of $\Delta\epsilon_1\Delta\epsilon_2$: minus - dashed line and plus - dotted line as well as for the "single-qubit" case [Eq. (37)] - solid line. In all plots $T = \Lambda/3$ and $s = 5$.

for a single qubit. More importantly, there is also a qualitatively new behavior here: Around the transit time $t = \tau$ there appears a characteristic disturbance in both the decoherence and fidelity plots. Weather it is a dip or a peak depends on the parity of $\Delta\epsilon_1\Delta\epsilon_2$. In the superradiant case ($\Delta\epsilon_1\Delta\epsilon_2 = +1$) it corresponds to a dip in the plotted curve, but a peak in the function $\Gamma_{\boldsymbol{\epsilon}\boldsymbol{\epsilon}'}(t)$ [we plot $-\ln\Gamma_{\boldsymbol{\epsilon}\boldsymbol{\epsilon}'}(t)$]; as expected, in this case the signal comes "in phase." Conversely, in the radiation trapping case ($\Delta\epsilon_1\Delta\epsilon_2 = -1$) it corresponds to a peak in the curve, but a dip in the function $\Gamma_{\boldsymbol{\epsilon}\boldsymbol{\epsilon}'}(t)$; as expected, in this case the signal comes "in antiphase." This behavior is due to a relaxation process where the qubits exchange a quantum of the bosonic field after the interaction has been switched on. It is basically a simpler version of the multiple retardation effects studied in the full model, with nontrivial qubit dynamics (see, e.g., [8,9]). There are no multiple signals here due to the trivial qubit Hamiltonian.

The disturbance is described by the vacuum part (see Appendix A), common to both decoherence and fidelity factors. More precisely, by the second term in (A2),

$$-\frac{\cos\{(s-1)\arctan[\Lambda(t-\tau)]\}}{[1 + \Lambda^2(t-\tau)^2]^{\frac{s-1}{2}}}. \qquad (41)$$

This term describes also the smaller disturbances, surrounding the main one in time, which appear for higher Ohmicity parameters s and $\Lambda\tau$ due to the cosine periodicity (see Fig. 1 for $\Lambda\tau = 5$). These disturbances indicate the breakdown of causality in our model for the time $\Lambda\tau \simeq 1$. As discussed, for instance, in [8,9], this is due to the introduction of the cut and causality is restored for longer times, or for all quantities for which the limit $\Lambda \rightarrow \infty$ has a mathematical sense.

The peaks in the plots for $\Delta\epsilon_1\Delta\epsilon_2 = -1$, i.e., for the pair of states $|\frac{1}{2}, -\frac{1}{2}\rangle, |-\frac{1}{2}, \frac{1}{2}\rangle$, imply that around $t = \tau$ both the decoherence factor and the overlap become small for this pair. This in turn implies that the partial state's projection onto the subspace spanned by $|\frac{1}{2}, -\frac{1}{2}\rangle, |-\frac{1}{2}, \frac{1}{2}\rangle$ approaches SBS [7]
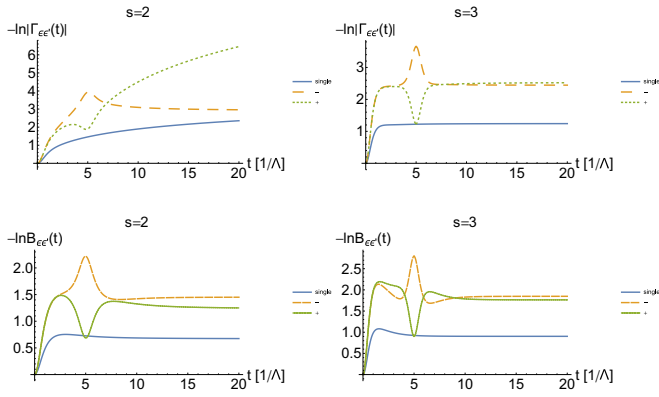
FIG. 2. Uncut spectral density case, different Ohmicity parameter. Logarithm of the decoherence factor [Eq. (39)] – upper trace, and fidelity [Eq. (40)] – lower trace for different values of Ohmicity parameter [Eq. (31)] s: $s = 2$ - upper left and lower left, $s = 3$ - upper right and lower right, which for a spin-boson model correspond to Markovian and non-Markovian evolution [21]. In each plot there are three curves corresponding to states with different values of $\Delta\epsilon_1\Delta\epsilon_2$: minus - dashed line and plus - dotted line as well as for the "single-qubit" case [Eq. (37)] - solid line. In all plots $T = \Lambda/3$ and $\Lambda\tau = 5$.
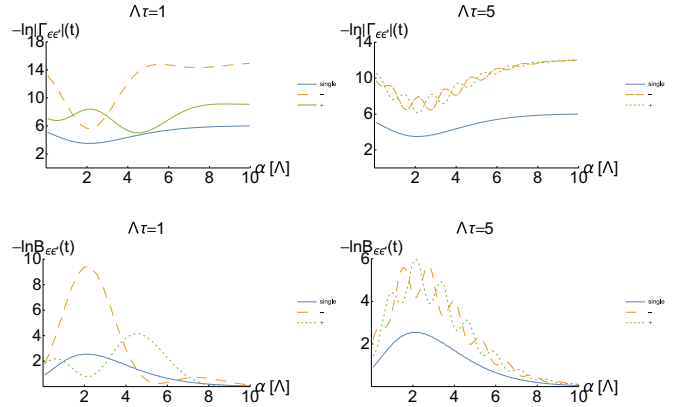

FIG. 3. Cut spectral density case. Time-asymptotic value of the decoherence factor [Eq. (39)] – upper trace, and fidelity [Eq. (40)] – lower trace as a function of the cut for different values of transit time τ [Eq. (26)]: $\Lambda\tau = 1$ - upper left and lower left, $\Lambda\tau = 5$ - upper right and lower right. In each plot there are three curves corresponding to states with different values of $\Delta\epsilon_1\Delta\epsilon_2$: minus - dashed line and plus - dotted line as well as for the "single qubit" case [Eq. (37)] - solid line. The unobserved frequencies belong to $(0, \alpha/\Lambda) \cup [(\alpha + \Delta)/\Lambda, \infty]$, whereas the observed ones to $[\alpha/\Lambda, (\alpha + \Delta)/\Lambda]$. In all plots $T = \Lambda/3$, $s = 5$, and $\Delta = 2$.

much better than at other times (a "blink of objectivity"):

$$\rho_{S:fE}^I(t = \tau) \approx \sum_{\epsilon=+-,-+} c_{\epsilon\epsilon}|\epsilon\rangle\langle\epsilon| \otimes \bigotimes_{\mathcal{M}} \rho_{\mathcal{M}}^I(\tau; \epsilon) + \text{rest}, \quad (42)$$

and $\rho_{\mathcal{M}}^I(\tau; 01)$ and $\rho_{\mathcal{M}}^I(\tau; 10)$ have a very small overlap. Contrarily, the dips for $\Delta\epsilon_1\Delta\epsilon_2 = +1$ signify that both decoherence and the overlap functions temporarily rise, indicating a departure from SBS and a form of a transient recoherence. As a result, the partially traced state has a rather complicated structure at around $t = \tau$, with parts well approximated by SBS and parts with restored quantum correlations. It thus, in a sense, simultaneously possesses classical (SBS) and quantum (coherences) properties.

In Fig. 1 we can also see the influence of the transit time. For low transit times compared to the cut-off timescale, both decoherence and fidelity curves split with the parity of $\Delta\epsilon_1\Delta\epsilon_2$. In particular, for the states with $\Delta\epsilon_1\Delta\epsilon_2 = -1$ the decoherence and the orthogonalization processes are more efficient, again bringing this part of $\rho_{S:fE}(t)$ closer to SBS than for those with $\Delta\epsilon_1\Delta\epsilon_2 = +1$. However, the asymptotic values for both cases are still higher than those for the single-qubit case. Increasing the value of the transit time to $\Lambda\tau = 5$, the differences in the time behavior of both parities $\Delta\epsilon_1\Delta\epsilon_2 = \pm 1$ almost disappear apart from the region around the transit time.

Next we investigate the influence of the Ohmicity parameter s [cf. Eq. (31)]. In Fig. 2 we present the behavior of decoherence and fidelity factors for $s = 2$ and $s = 3$. This corresponds to a well-known transition between the Markovian and non-Markovian evolution of the single-spin model and manifests in the change from monotonic to nonmonotonic behavior of the single-spin decoherence curve [21,22]. In the case of the spin register, one can see that already for $s = 2$

the decoherence curves are nonmonotonic (for off-diagonal elements with $\Delta\epsilon_1\Delta\epsilon_2 = \pm 1$) due to the relaxation process around $t = \tau$, and there is no qualitative change between $s = 2$ and $s = 3$. Comparing Figs. 2 and 1, one sees that the peak and/or dip becomes more pronounced with increasing the Ohmicity parameter, but the differences between the decoherence and the fidelity curves disappear for the chosen temperature $T = \Lambda/3$. Finally, let us mention that a relation between non-Markovianity and efficiency of SBS formation was studied for a single-spin model in [6] and no direct connection between the two processes was found. Let us also mention that a quantification of non-Markovianity here would require introduction of an appropriate, for the studied model, non-Markovianity measure [23].

We now move to the cut spectral density case (cf. [6]). We assume that the observed frequencies belong to a window $[\alpha/\Lambda, (\alpha + \Delta)/\Lambda]$ and the complement of this interval is not observed (the traced-out part of the bosonic environment). In Fig. 3 we present time-asymptotic ($\Lambda t \gg 1$) values of decoherence and fidelity factors as functions of the cut position α and for different transit times. Although the behavior is much more complicated than for a single spin, one can still see a characteristic reciprocal behavior [6] between decoherence (upper plots) and fidelity (lower plots) factors, reflecting reciprocal dependence on the temperature of the two functions. In addition, one observes small oscillations of both fidelity and decoherence factor for states with $\Delta\epsilon_1\Delta\epsilon_2 = \pm 1$ with respect to the placement of the cut. We verified that for higher values of transit time these oscillations vanish, so that there is no difference in decoherence and fidelity between states with $\Delta\epsilon_1\Delta\epsilon_2 = \pm 1$. For transit times $\Lambda\tau \gg 1$ the "single-qubit" case results in weaker decoherence and information transfer to the environment than the other two discussed cases.

V. COLLECTIVE DECOHERENCE AND ORTHOGONALIZATION

Looking at the exact expressions for the uncut (the whole environment traced out) case in Appendix A, one sees that the transit times τ_{nm} always scale with other time constants: the cut-off frequency Λ and the thermal time $\tau_T = 1/(k_B T)$. Let us now consider the situation when τ_{mn} values are the shortest timescales in the model:

$$\tau_{nm} \ll \tau_T, \Lambda^{-1} \qquad (43)$$

for all n, m. In particular, the last condition is equivalent through (26) to that of the qubit separation being much smaller than the wavelengths involved, $k\Delta r_{nm} \ll 1$, or that the coupling constants do not depend on the qubit positions:

$$g_k^n \equiv g_k. \qquad (44)$$

From (15) and (24) it follows that

$$-\ln \Gamma_{\epsilon\epsilon'}(t) = \mathbf{\Gamma}_{11}(t)\left(\sum_n \Delta\epsilon_n\right)^2 \qquad (45)$$

$$+i\mathbf{\Gamma}_{11}^+(t)\left[\left(\sum_n \epsilon_n\right)^2 - \left(\sum_n \epsilon_n'\right)^2\right] \qquad (46)$$

and

$$-\ln B_{\epsilon\epsilon'}^{\mathcal{M}}(t) = \mathbf{B}_{11}^{\mathcal{M}}(t)\left(\sum_n \Delta\epsilon_n\right)^2. \qquad (47)$$

The quantities $\mathbf{\Gamma}_{11}(t)$, $\mathbf{B}_{11}^{\mathcal{M}}(t)$ are just the single-qubit ($L = 1$) decoherence and distinguishability factors, analyzed, e.g., in [6]. Hence, in this regime the whole register behaves almost like a collection of independent qubits, with the important qualitative difference of existence of DFS and OFS (see Sec. III). In particular, a simultaneous strong DFS and OFS occur for all pairs ϵ, ϵ' such that (cf. [2])

$$\sum_n \Delta\epsilon_n = \sum_n (\epsilon_n - \epsilon_n') = 0, \qquad (48)$$

$$\left(\sum_n \epsilon_n\right)^2 - \left(\sum_n \epsilon_n'\right)^2 = 0, \qquad (49)$$

while a simultaneous weak DFS and OFS occur when only (48) is fulfilled. It is interesting that the same condition (48) controls both decoherence and state fidelity. An example of a simultaneous strong DFS and OFS is the subspace of a two-qubit register spanned by $|\frac{1}{2}, -\frac{1}{2}\rangle$ and $|-\frac{1}{2}, \frac{1}{2}\rangle$ (analyzed in more detail in [2]). On the other hand, the pairs of states that decohere most and become most distinguishable are those for which $\sum_n \Delta\epsilon_n$ is the largest.

Let us investigate the structure of the partially reduced state in the presence of a simultaneous strong DFS and OFS. Let us denote this subspace as DFS and assume it to be strong. For the sake of clarity, we consider it to be two-dimensional, spanned by vectors $\tilde{\epsilon}$, $\tilde{\epsilon}'$ (the extension to higher dimensions is analogous). We find that [cf. Eq. (8)]

$$\hat{U}_k(t; \tilde{\epsilon}) = \hat{U}_k(t; \tilde{\epsilon}'), \qquad (50)$$

which can be immediately verified using Eqs. (48) and (49):

$$U_k^I(t; \tilde{\epsilon})^\dagger U_k^I(t; \tilde{\epsilon}) = \hat{D}\left(\alpha_k(t)g_k \sum_n \Delta\epsilon_n\right)$$

$$\times\, e^{ig_k[(\sum_n \epsilon_n)^2 - (\sum_n \epsilon_n')^2]\xi_k(t)} = I. \qquad (51)$$

As a result, the controlled unitary operator has a form

$$\hat{U}_{S:E}^I(t) = \hat{\Pi}_{\mathrm{DFS}} \otimes \bigotimes_k^{fN} \hat{U}_k^I(t; \mathrm{DFS})$$

$$+ \sum_{\epsilon \notin \mathrm{DFS}} |\epsilon\rangle\langle\epsilon| \otimes \bigotimes_k^{fN} \hat{U}_k^I(t; \epsilon), \qquad (52)$$

where $\hat{\Pi}_{\mathrm{DFS}}$ is a projector onto DFS, i.e.,

$$\hat{\Pi}_{\mathrm{DFS}} = |\tilde{\epsilon}\rangle\langle\tilde{\epsilon}| + |\tilde{\epsilon}'\rangle\langle\tilde{\epsilon}'| + |\tilde{\epsilon}\rangle\langle\tilde{\epsilon}'| + |\tilde{\epsilon}'\rangle\langle\tilde{\epsilon}|. \qquad (53)$$

Let us assume that the conditions for formation of SBS are fulfilled for register states not belonging to DFS, so then the partially reduced state is

$$\rho_{S:fE}^I = \hat{\Pi}_{\mathrm{DFS}}\rho_{0S}\hat{\Pi}_{\mathrm{DFS}} \otimes \bigotimes_{\mathcal{M}}^{f\mathcal{M}} \rho_{\mathcal{M}}^I(t; \mathrm{DFS})$$

$$+ \sum_{\epsilon \notin \mathrm{DFS}} c_{\epsilon,\epsilon} |\epsilon\rangle\langle\epsilon| \otimes \bigotimes_{\mathcal{M}}^{f\mathcal{M}} \rho_{\mathcal{M}}^I(t; \epsilon). \qquad (54)$$

This is what we call a coarse-grained SBS [7]: The SBS structure is build upon subspaces rather than states (the pointer states), and coherences are generally preserved within the subspaces, and the information leaked into the environment allows discrimination only between subspaces but not between the vectors they are spanned on. Further studies on various forms of departure from SBS can be found in [7].

VI. CONCLUSIONS

We revisited the decoherence process of a multiqubit register interacting with a bosonic thermal bath. Unlike in the previous studies [1,2], we were interested in information gained by the environment. To this end, we employed a recently introduced notion of spectrum broadcast structures (SBS) [4,5], which are specific multipartite quantum state structures describing redundant encoding of system information (here the register state) in the environment. We explicitly calculated the relevant figures of merit describing the SBS formation—the usual decoherence factor and mixed state fidelities—in the simple case of a so-called uncut environment, where each observer observing the environment has access to the full frequency spectrum. Studying in more detail the simplest case of a two-qubit register, we pointed to the causal disturbance propagation between the qubits, which can de- or recohere the register state, depending on its parity. Although this was previously known at the level of the register state [2,8,9], here we showed that there is an accompanying impulse in the environment causing an increase or decrease of environment information, respectively. In another simple case of collective decoherence corresponding to vanishingly small transit times of the field disturbance between the qubits,

we showed a coarse-grained SBS. These are quite interesting structures, appearing in the presence of protected spaces.

The model considered here was quite simple with a trivial dynamics of the register. One future direction would be studies of a more realistic full model, which includes register tunneling [8,9]. However, already at the sole central system level the dynamics is rich and complicated, e.g., with multiple causal impulses propagating between the qubits.

Moreover, let us further elaborate on the link between the dynamics of the multiqubit register and Dicke superradiance. The standard picture of decay of unstable states, such as occurs in Dicke superradiance, is that the first radiated photons are completely spontaneous and random and then the signal amplifies and becomes classical—e.g., it can be described to a high degree of accuracy by coherent states [24], closely resembling properties of classical states. This way of achieving "classicality" may likely be a mechanism of SBS formation. Classical states achieved in such processes are very random since they result from amplification of the spontaneous initial part of radiation. Therefore, this process is usually regarded as a manifestation of macroscopic quantum fluctuations [25,26]. It would be very interesting to use a multiqubit register to investigate this problem from an SBS perspective, and we leave this for a further study.

APPENDIX A: UNCUT ENVIRONMENT – ANALYTICAL FORMULAS

In this Appendix we provide an analytical expression for decoherence factor and mixed state fidelity. As in the main text, we assume that the spectral density is given by the following expression:

$$J(\omega) = \frac{\omega^s}{\Lambda^{s-1}} \exp[-\omega/\Lambda], \tag{A1}$$

with $s > 1$. As usual [19,20], the decoherence factor factorizes into the vacuum and thermal parts, $\mathbf{\Gamma}(t) = \mathbf{\Gamma}^{\mathrm{vac}}(t) + \mathbf{\Gamma}^{th}(t)$, which in the considered model is

$$\mathbf{\Gamma}_{nm}^{\mathrm{vac}}(t)$$
$$= \frac{\wp(s-1)}{2}\Big[2[1 + (\Lambda\tau_{nm})^2]^{\frac{1-s}{2}}\cos[(s-1)\arctan(\Lambda\tau_{nm})]$$
$$- [1 + (\Lambda t_{nm}^-)^2]^{\frac{1-s}{2}}\cos[(s-1)\arctan(\Lambda t_{nm}^-)]$$
$$- [1 + (\Lambda t_{nm}^+)^2]^{\frac{1-s}{2}}\cos[(s-1)\arctan(\Lambda t_{nm}^+)]\Big], \tag{A2}$$

$$\mathbf{\Gamma}_{nm}^{th}(t) = \frac{(-1)^{s-1}}{(\Lambda\tau_T)^{s-1}}\Bigg[2\Psi^{(s-2)}\bigg(1 + \frac{1}{\Lambda\tau_T} + i\frac{\tau_{nm}}{\tau_T}\bigg)$$
$$- \Psi^{(s-2)}\bigg(1 + \frac{1}{\Lambda\tau_T} - \frac{it_{nm}^+}{\tau_T}\bigg)$$
$$- \Psi^{(s-2)}\bigg(1 + \frac{1}{\Lambda\tau_T} - \frac{it_{nm}^-}{\tau_T}\bigg) + \text{c.c.}\Bigg], \tag{A3}$$

where $\Psi^m(z)$ is the so-called polygamma function, defined as [27]

$$\Psi^m(z) \equiv \frac{d^{m+1}}{dz^{m+1}}\ln\wp(z) = \sum_{k=0}^{\infty}\frac{(-1)^{m+1}m!}{(z+k)^{m+1}}, \tag{A4}$$

$\wp(z)$ is the Euler gamma function, c.c. denotes complex conjugated part, we introduced advanced and retarded times,

$$t_{nm}^{\pm} \equiv t \pm \tau_{nm}, \tag{A5}$$

and $\tau_T = 1/(k_B T)$. The quantities entering the phases are

$$\mathbf{\Gamma}_{nm}^{+}(t) = \frac{\wp(s-1)}{2}\Big[2(s-1)\Lambda t[1 + (\Lambda\tau_{nm})^2]^{-\frac{s}{2}}$$
$$\times \cos[s\arctan(\Lambda\tau_{nm})].$$
$$- [1 + (\Lambda t_{nm}^-)^2]^{\frac{1-s}{2}}\sin[(s-1)\arctan(\Lambda t_{nm}^-)]$$
$$- [1 + (\Lambda t_{nm}^+)^2]^{\frac{1-s}{2}}\sin[(s-1)\arctan(\Lambda t_{nm}^+)]\Big], \tag{A6}$$

$$\mathbf{\Gamma}_{nm}^{-}(t) = \frac{\wp(s-1)}{2}\Big[2[1+(\Lambda\tau_{nm})^2]^{\frac{1-s}{2}}\sin[(s-1)\arctan(\Lambda t_{nm})]$$
$$+ [1 + (\Lambda t_{nm}^-)^2]^{\frac{1-s}{2}}\sin[(s-1)\arctan(\Lambda t_{nm}^-)]$$
$$+ [1 + (\Lambda t_{nm}^+)^2]^{\frac{1-s}{2}}\sin[(s-1)\arctan(\Lambda t_{nm}^+)]\Big]. \tag{A7}$$

Distinguishability can also be decomposed into a vacuum and thermal part $\mathbf{B}^{\mathcal{M}}(t) = \mathbf{B}^{\mathcal{M}\,\mathrm{vac}}(t) + \mathbf{B}^{\mathcal{M}\,th}(t)$, with $\mathbf{B}^{\mathcal{M}\,\mathrm{vac}}(t) = \mathbf{\Gamma}^{\mathrm{vac}}(t)$ and

$$\mathbf{B}_{nm}^{\mathcal{M}\,th}(t) = \frac{(-1)^{s-1}}{(2\Lambda\tau_T)^{s-1}}\Bigg[\Psi^{(s-2)}\bigg(1 + \frac{1}{2\Lambda\tau_T} + \frac{i\tau_{nm}}{2\tau_T}\bigg)$$
$$- \Psi^{(s-2)}\bigg(\frac{1}{2} + \frac{1}{2\Lambda\tau_T} + \frac{it_{nm}}{2\tau_T}\bigg)$$
$$- \frac{1}{2}\Psi^{(s-2)}\bigg(1 + \frac{1}{2\Lambda\tau_T} - \frac{it_{nm}^+}{2\tau_T}\bigg)$$
$$+ \frac{1}{2}\Psi^{(s-2)}\bigg(\frac{1}{2} + \frac{1}{2\Lambda\tau_T} - \frac{it_{nm}^+}{2\tau_T}\bigg)$$
$$- \frac{1}{2}\Psi^{(s-2)}\bigg(1 + \frac{1}{2\Lambda\tau_T} - \frac{it_{nm}^-}{2\tau_T}\bigg)$$
$$+ \frac{1}{2}\Psi^{(s-2)}\bigg(\frac{1}{2} + \frac{1}{2\Lambda\tau_T} - \frac{it_{nm}^-}{2\tau_T}\bigg) + \text{c.c.}\Bigg]. \tag{A8}$$

APPENDIX B: SUPERRADIANCE AND RADIATION TRAPPING

In 1954 Dicke [10] predicted that N emitters and/or dipoles will radiate collectively with the rate proportional to N and

intensity proportional to N^2, provided they are confined in a region of a size much smaller than λ^D in D dimensions, where λ is the wavelength of the radiation. Only one mode of such systems, the one in which all dipoles are parallel and have the same phase, will exhibit collective superradiance. All the other modes, with the total dipole moment equal to zero, will be nonradiative, or in practice will radiate very slowly. Since the famous paper of Dicke, a lot of work has been done on collective emission from a system of many sources. In the 1970s and 1980s the theory focused more on superfluorescence and considered usually pencil-shape samples, of dimensions large compared with the wavelength, for which propagation effects play a dominant role (e.g., [25,28,29]). It was widely believed that in a small sample limit the original Dicke's description is valid. Namely, in such a limit, only a global dipole moment is coupled to the radiation; the lifetime of the excitation of this degree of freedom is N times shorter than the lifetime of a single atom and the excitations of all the other global modes of the system are trapped and cannot decay through radiative damping. This simple picture can be inadequate due to near-zone effects, as was suggested in the paper of

Friedberg and Hartmann [30,31], which dealt with a small spherical sample. This problem was studied for the spherical sample composed of charged harmonic oscillators by [32]. Essential for these studies was taking into account the near-zone field in the system, and longitudinal dipole-dipole forces in particular.

On the other hand, there are a lot of papers studying the problem of two atoms [8,33,34]. In fact, it is known from the paper of Stephen [35] that proper collective broadening and narrowing of the emission line conform to a simple picture developed by Dicke. In contrast, in Ref. [36] it was shown that Dicke's superradiance, strictly speaking, ceases to exist in a system of four atoms (harmonic oscillators) located on the vertices of a tetrahedron or equilateral triangle. This effect results from the mode mixing due to the strong near-zone interactions at short distances, smaller than the wavelength.

Recently, there has been a revival of interest in radiation trapping and collective emission in the context of quantum nanophotonics [37]. Here, the mechanisms of radiation trapping are more subtle and are governed by destructive interference patterns.

[1] G. M. Palma, K.-A. Suominen, and A. K. Ekert, Quantum computers and dissipation, Proc. R. Soc. London A **452**, 567 (1996).

[2] J. H. Reina, L. Quiroga, and N. F. Johnson, Decoherence of quantum registers, Phys. Rev. A **65**, 032326 (2002).

[3] W. H. Zurek, Quantum darwinism, Nat. Phys. **5**, 181 (2009).

[4] J. K. Korbicz, P. Horodecki, and R. Horodecki, Objectivity in a Noisy Photonic Environment Through Quantum State Information Broadcasting, Phys. Rev. Lett. **112**, 120402 (2014).

[5] R. Horodecki, J. K. Korbicz, and P. Horodecki, Quantum origins of objectivity, Phys. Rev. A **91**, 032122 (2015).

[6] A. Lampo, J. Tuziemski, M. Lewenstein, and J. K. Korbicz, Objectivity in the non-Markovian spin-boson model, Phys. Rev. A **96**, 012120 (2017).

[7] P. Mironowicz, P. Należyty, P. Horodecki, and J. K. Korbicz, System information propagation for spin structures, Phys. Rev. A **98**, 022124 (2018).

[8] P. W. Milonni and P. L. Knight, Retardation in the resonant interaction of two identical atoms, Phys. Rev. A **10**, 1096 (1974).

[9] K. Rzążewski and W. Żakowicz, Initial value problem and causality of radiating oscillator, J. Phys. A **9**, 1159 (1976).

[10] R. H. Dicke, Coherence in spontaneous radiation processes, Phys. Rev. **93**, 99 (1954).

[11] J. Tuziemski and J. K. Korbicz, Objectivisation in simplified quantum Brownian motion models, Photonics **2**, 228 (2015).

[12] J. Tuziemski and J. K. Korbicz, Dynamical objectivity in quantum Brownian motion, EPL **112**, 40008 (2015).

[13] J. Tuziemski and J. K. Korbicz, Analytical studies of spectrum broadcast structures in quantum Brownian motion, J. Phys. A: Mathematical and Theoretical **49**, 445301 (2016).

[14] J. Tuziemski, P. Witas, and J. K. Korbicz, Redundant information encoding in QED during decoherence, Phys. Rev. A **97**, 012110 (2018).

[15] J. K. Korbicz and J. Tuziemski, Information transfer during the universal gravitational decoherence, Gen. Relativ. Gravit. **49**, 152 (2017).

[16] J. K. Korbicz, E. A. Aguilar, P. Ćwikliński, and P. Horodecki, Generic appearance of objective results in quantum measurements, Phys. Rev. A **96**, 032124 (2017).

[17] P. Mironowicz, J. K. Korbicz, and P. Horodecki, Monitoring of the Process of System Information Broadcasting in Time, Phys. Rev. Lett. **118**, 150501 (2017).

[18] C. A. Fuchs and J. van de Graaf, Cryptographic distinguishability measures for quantum-mechanical states, IEEE Trans. Inf. Theory **45**, 1216 (1999).

[19] M. A. Schlosshauer, *Decoherence and the Quantum-To-Classical Transition*, The Frontiers Collection (Springer-Verlag, Berlin, Heilderberg, 2007).

[20] H. P. Breuer and F. Petruccione, *The Theory of Open Quantum Systems* (Oxford University Press, Oxford, 2007).

[21] C. Addis, B. Bylicka, D. Chruściński, and S. Maniscalco, Comparative study of non-Markovianity measures in exactly solvable one- and two-qubit models, Phys. Rev. A **90**, 052103 (2014).

[22] H.-P. Breuer, E.-M. Laine, J. Piilo, and B. Vacchini, *Colloquium*: Non-Markovian dynamics in open quantum systems, Rev. Mod. Phys. **88**, 021002 (2016).

[23] M. J. W. Hall, J. D. Cresser, L. Li, and E. Andersson, Canonical form of master equations and characterization of non-Markovianity, Phys. Rev. A **89**, 042120 (2014).

[24] F. T. Arecchi, E. Courtens, R. Gilmore, and H. Thomas, Atomic coherent states in quantum optics, Phys. Rev. A **6**, 2211 (1972).

[25] F. Haake, H. King, G. Schröder, J. Haus, and R. Glauber, Fluctuations in superfluorescence, Phys. Rev. A **20**, 2047 (1979).

[26] F. Haake, H. King, G. Schröder, J. Haus, R. Glauber, and F. Hopf, Macroscopic Quantum Fluctuations in Superfluorescence, Phys. Rev. Lett. **42**, 1740 (1979).

[27] DLMF, NIST Digital Library of Mathematical Functions, http://dlmf.nist.gov/, Release 1.0.20 of 2018-09-15, edited by f. W. J. Olver, A. B. Olde Daalhuis, D. W. Lozier, B. I. Schneider, R. F. Boisvert, C. W. Clark, B. R. Miller, and B. V. Saunders.

[28] G. Banfi and R. Bonifacio, Superfluorescence and cooperative frequency shift, Phys. Rev. A **12**, 2068 (1975).

[29] R. Bonifacio, P. Schwendimann, and F. Haake, Quantum statistical theory of superradiance, I, Phys. Rev. A **4**, 302 (1971).

[30] R. Friedberg and S. R. Hartmann, Superradiant stability in specially shaped small samples, Opt. Commun. **10**, 298 (1974).

[31] R. Friedberg and S. R. Hartmann, Temporal evolution of superradiance in a small sphere, Phys. Rev. A **10**, 1728 (1974).

[32] W Żakowicz, Superradiant decay of a small spherical system of harmonic oscillators, Phys. Rev. A **17**, 343 (1978).

[33] G. S. Agarwal, A. C. Brown, L. M. Narducci, and G. Vetri, Collective atomic effects in resonance fluorescence, Phys. Rev. A **15**, 1613 (1977).

[34] M. Kuś and K. Wódkiewicz, Two-atom resonance fluorescence, Phys. Rev. A **23**, 853 (1981).

[35] M. J. Stephen, First-order dispersion forces, J. Chem. Phys. **40**, 669 (1964).

[36] M. Lewenstein and K. Rzazewski, Collective radiation and the near-zone field, J. Phys. A: Math. Gen. **13**, 743 (1980).

[37] A. Asenjo-Garcia, M. Moreno-Cardoner, A. Albrecht, H. J. Kimble, and D. E. Chang, Exponential Improvement in Photon Storage Fidelities Using Subradiance and "Selective Radiance" in Atomic Arrays, Phys. Rev. X **7**, 031024 (2017).